

Effects of a Non-Ideal Plane Wave on Compact Range Measurements

David Wayne, Jeffrey A. Fordham, John McKenna

MI Technologies

Suwanee, Georgia, USA

dwayne@mitechnologies.com

jfordham@mitechnologies.com

jmckenna@mitechnologies.com

Abstract— Performance requirements for compact ranges are typically specified as metrics describing the quiet zone's electromagnetic-field quality. The typical metrics are amplitude taper and ripple, phase variation, and cross polarization. Acceptance testing of compact ranges involves field probing of the quiet zone to confirm that these metrics are within their specified limits. It is expected that if the metrics are met, then measurements of an antenna placed within that quiet zone will have acceptably low uncertainty. However, a literature search on the relationship of these parameters to resultant errors in antenna measurement yields limited published documentation on the subject.

Various methods for determining the uncertainty in antenna measurements have been previously developed and presented for far-field and near-field antenna measurements. An uncertainty analysis for a compact range would include, as one of its terms, the quality of the field illuminating on the antenna of interest. In a compact range, the illumination is non-ideal in amplitude, phase and polarization. Error sources such as reflector surface inaccuracies, chamber-induced stray signals, reflector and edge treatment geometry, and instrumentation RF leakage, perturb the illumination from ideal.

This paper will review, in a summary fashion, the equations that estimate the effect of a non-ideal incident electromagnetic field on an antenna. It will calculate the resulting antenna pattern for a candidate antenna and compare it to the ideal antenna pattern thus showing the induced errors. Parametric studies will be presented studying the error effects of varying illumination metrics on the antenna measurement. In addition, measured field probe data from a compact range will also be used with the candidate antennas to investigate induced errors.

The intent is to provide the reader with insight as to how the typical compact range metrics affect the accuracy of an antenna measurement. This work is intended to be the foundation for future work to develop a comprehensive uncertainty analysis for compact range measurements.

Keywords: Compact Range, Antenna Measurement Uncertainties, plane wave quality

I. INTRODUCTION

When measuring an antenna pattern, the following parameters are usually of interest:

- Gain (dB_i)
- 3 dB Beam Width
- Peak Side Lobe Level (dB_c)

When measuring the quality of a compact range quiet zone (QZ), the following metrics of the incident field are typically used [1] Section 14.3:

- Amplitude Ripple
- Phase Variation
- Amplitude Taper

The intent of this paper is to show a method to estimate antenna pattern parameter uncertainty from a specified QZ metric or to estimate expected antenna pattern parameter error from actual QZ field probe data, this for a given ideal or expected antenna pattern.

- (A) You have an expected antenna pattern and a QZ specified in terms of field probe metrics. How to calculate the uncertainty.
- (B) You have an expected antenna pattern and measured or simulated QZ field data. How to calculate the expected error.

The effect of extraneous stray signals or amplitude taper in the far field on an antenna pattern is well described in sections 14.2 and 14.3 of reference [1]. The subject of the effects upon antenna pattern measurements from the predicted quiet zone fields from a compact range reflector was discussed by Lee and Burnside [2]. However, the relationship of compact range field probe metrics to these parameters and therefore to antenna parameters is not as well discussed and therefore is the subject of this paper.

II. FORMULATION

This section of this paper will present equations estimating the effect of an incident electromagnetic field on an antenna.

First consider if a receiving antenna with radiation pattern $R(\theta, \phi)$ is immersed in the field of plane waves from N directions (Figure 1),

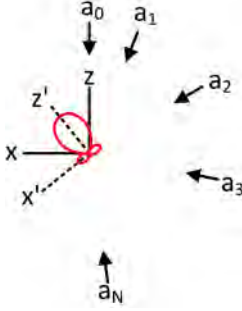


Figure 1. AUT rotated within a fixed constellation of plane waves.

then the measured response M at an antenna positioner angle (θ, ϕ) is

$$M(\theta, \phi) = \sum_{i=0}^{N-1} a_i R(x'_i, y'_i, z'_i) \quad (1)$$

where a_i are complex coefficients representing amplitude and phase of the associated illuminating plane wave. R is evaluated in the antenna's frame of reference, indicated by primed coordinates. To facilitate the R evaluation, the primed coordinates are expressed in terms of the unprimed via the rotation matrix \mathcal{R}

$$\begin{bmatrix} x' \\ y' \\ z' \end{bmatrix} = [\mathcal{R}] \begin{bmatrix} x \\ y \\ z \end{bmatrix} \quad (2)$$

where \mathcal{R} takes the form, for a roll-over azimuth positioner,

$$\mathcal{R} = \begin{bmatrix} \cos \phi \cos \theta & \sin \phi & -\cos \phi \sin \theta \\ -\sin \phi \cos \theta & \cos \phi & \sin \phi \sin \theta \\ \sin \theta & 0 & \cos \theta \end{bmatrix} \quad (3)$$

Commonly the single plane a_0 wave illuminates from $(x_0, y_0, z_0) = (0, 0, 1)$, or equivalently $(\theta_0, \phi_0) = (0, 0)$ and (1) reduces to

$$M(\theta, \phi) = a_0 R(\theta, 180 - \phi) \quad (4)$$

Equation (1) is valid for the general case of illumination from any direction. If a restriction is made to constrain the antenna under test to a fixed position (i.e., not rotating in the

QZ), then reference [2] offers the following equation where M is expressed (see Figure 2). We will consider this simplification acceptable for our purpose.

$$M(\theta, \phi) = \sum_{m=-M}^M \sum_{n=-N}^N Q_{m,n} \frac{I_{m,n}}{I_{0,0}} \times \left[e^{jkx_m (\sin \theta \cos \phi - \sin \theta_s \cos \phi_s)} \right] \times \left[e^{jky_n (\sin \theta \sin \phi - \sin \theta_s \cos \phi_s)} \right] \quad (5)$$

in which

- $Q_{m,n}$ complex amplitude of Quiet Zone illumination at location x_m, y_n ;
- $I_{m,n}$ complex total current at the "terminals" of the m, n th radiator
- X_m x-coordinate of a column of radiators, $x_m = md_x$;
- Y_n y-coordinate of a row of radiators, $y_n = nd_y$;
- θ_s, ϕ_s direction of the electronically-steered main pencil beam;
- k $k = \omega/c = 2\pi/\lambda$ is the wave number.

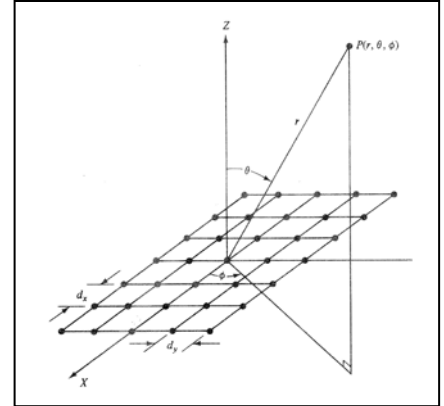


Figure 2. Planar Array: elements arranged in a Rectangular Grid

Equation (5) is the vehicle through which we conduct a study presented in the remainder of the paper. We will construct Q using QZ metrics of interest and then construct Q from measured field probe data. We will construct I from the aperture distribution of an example antenna.

III. ANTENNA EXAMPLE

An antenna is chosen that is representative of one suitable for testing in a compact range. Its pattern, when illuminated with a perfect plane wave, is calculated using a simulation based on Equation (5). Then it is recalculated with QZ imperfections added and compared.

The antenna chosen is a $33\lambda \times 17\lambda$ planar array containing an aperture excitation I, computed as a -35 dB Taylor, NBAR=6 and a $Q_{m,n} = 1$ (uniform plane wave illumination). Running the simulation produces the expected antenna pattern shown in Figure 3 and the parameters listed below:

- Gain (dB_c) 36.0
- 3 dB Beam Width (Az/EL) 2.10/4.28
- Peak Sidelobe Level (dB_c) -35.4

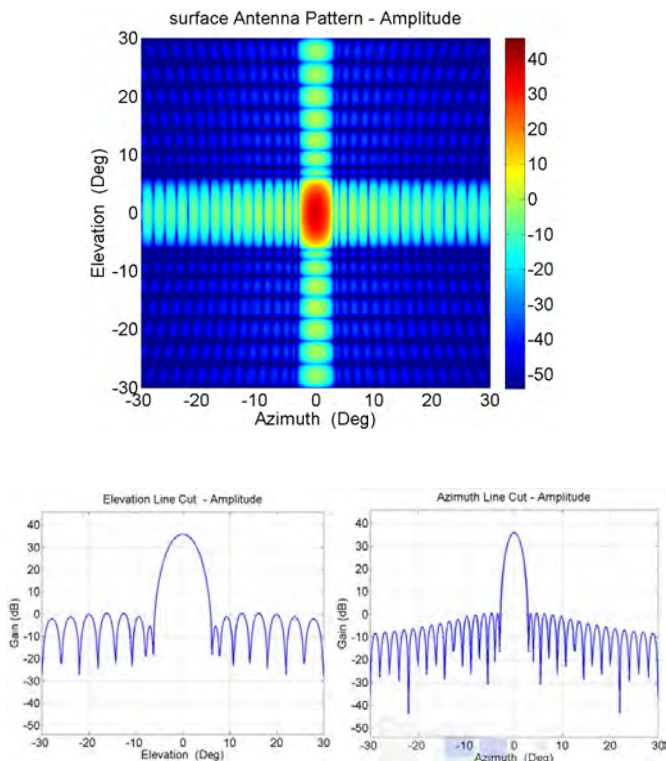


Figure 3. Equation (5); 2.5 GHz 4 X 2 m array, 35 dB Taylor NBAR=6; perfect QZ

It is desired to add QZ imperfections to the plane wave and generate similar plots as Figure 3. Imperfections in the QZ are a function of stray signals from multiple directions which contributes amplitude and phase variations. For the purposes of the simulations in this paper, the relationship is discussed as follows.

The Phase Variation PV is derived from a field probe trace by measuring the full excursion of the phase over the aperture of the quiet zone. Amplitude ripple σ is the difference in decibels between maxima and minima. Consider Figure 4.

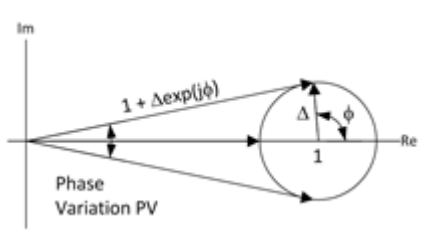


Figure 4. Relationship between Phase Variation PV & Amplitude Ripple

Δ and σ are related through [reference [1] eq 14.84].

$$\Delta = \frac{\sigma}{10^{\frac{\sigma}{20}} - 1} \tag{6}$$

In Figure 4, ϕ represents the relative phase of a stray signal source.

For small σ , say $0 \leq \sigma \leq 1$ dB, $\Delta \ll 1$. The small angle approximation applies, $\sin(PV) \sim PV$ radians, and the geometry of Figure 4 yields $PV = 2 \Delta$ (radians).

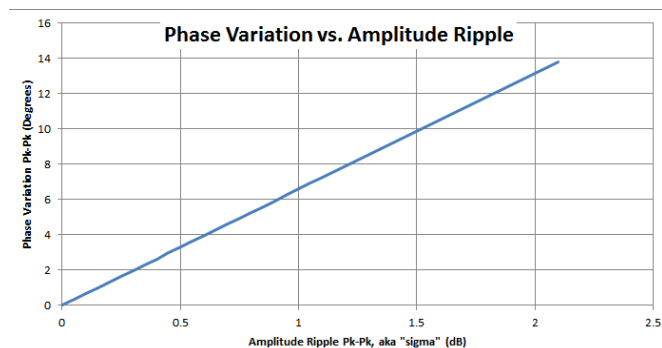


Figure 5 At small amplitude, Phase Variation Δ and Amplitude Ripple σ

For example in the use of Figure 5, if the QZ ripple σ is 0.5 dB, then the resulting Phase Variation PV is ~ 3.5 degrees.

IV. PARAMETRIC STUDY OF EFFECTS OF NON IDEAL PLANE WAVE

An amplitude ripple is introduced using a value of 1.0 dB_{p-p} that might be specified for a typical compact range. It has a corresponding phase variation of 6.4 Degrees (Figure 5). The ripple was modeled as a single stray signal coming from an angle off the horizontal axis. The source of the stray signal was set initially off axis at an angle commensurate with the 6th null position (NBAR 6) of the ideal Taylor pattern and then walked in toward the main beam at each null position (NBAR 5 to 0). Figure 6 clearly shows the stray signal manifests itself in the pattern as a side lobe. As the angle of arrival lessens the induced side lobe moves toward the main beam. Only when it nears the main beam does it affect the 3 dB beam width of the pattern. As it overlaps the beam it affects the gain measurement of the pattern.

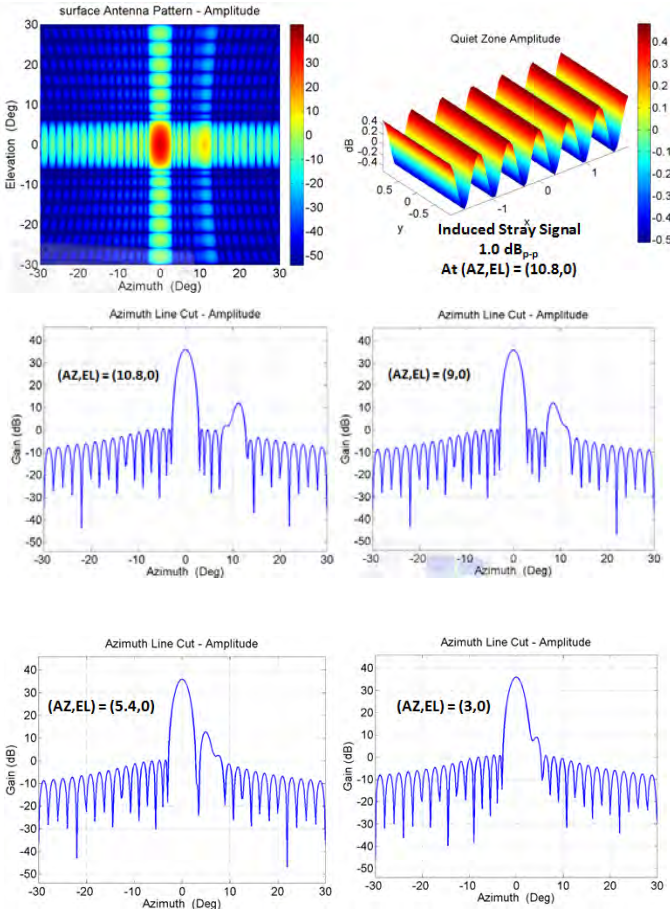


Figure 6. Walking Stray Signal from off Axis to Main Center

Upon study these are not unexpected results for a far field range, but they do provide a perspective in the context of compact range metrics. We see the stray signal causing significant error when measuring the side lobes. We see that an amplitude ripple specification of 1.0 dB_{p-p} is inadequate, by its self, to protect us from this error. In reality, the non-ideal plane wave measured by probing in a compact range is a mosaic of signals. A 1.0 dB_{p-p} amplitude ripple specification is a maximum allowable number anywhere in the QZ but it rarely exists throughout the QZ. The ramifications of this will be discussed more in Section VII.

V. CALCULATING THE UNCERTAINTY BOUND

The previous discussion introduced a stray signal in terms of amplitude ripple from specific directions. A more generalized view can be obtained by selecting amplitude ripple values of interest and using equation 14.55 in reference [1] to calculate the corresponding extraneous stray signal value.

$$\Delta L = 20 \log[(e_D + e_X)/e_D] \quad (6)$$

where,

e_D is the voltage at any point in an ideal or expected antenna pattern. In our example, these values were calculated in section III.

e_X is an extraneous signal. In our example it is the QZ amplitude ripple value of interest.

ΔL is the calculated error which can be applied to any point in the idealized (expected) pattern.

The plots in Figure 7 show the maximum uncertainty associated with a single stray signal of unknown spatial origin. The uncertainty bounds are calculated in this way by superimposing upon the ideal antenna pattern, the stray signal corresponding to ripple values of interest, ranging from 0.1, 0.54 to 0.79 dB_{p-p}. The later 2 values are field probe measurements taken from a typical compact range that is discussed later in Section VII

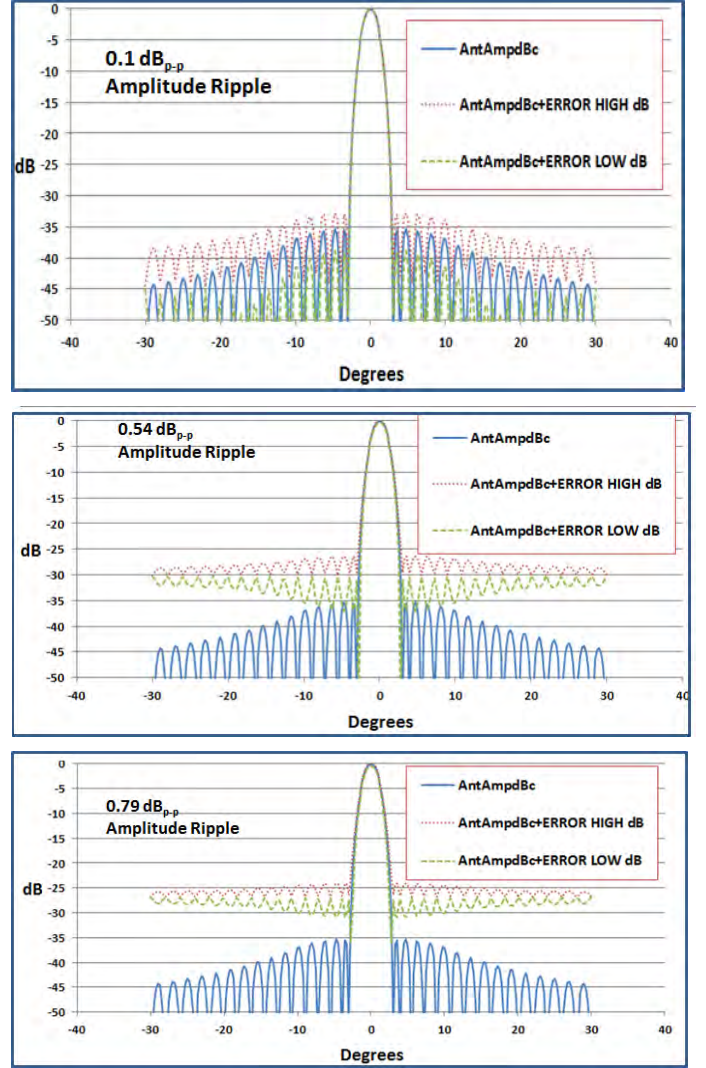


Figure 7. Maximum Uncertainty Bounds Due to Amplitude Ripple in the QZ Field

The plots show that when stray signals are introduced at levels commensurate with typical QZ field probe metrics (0.59 & 0.79 dB_{p-p}), significant error in side lobe measurements are possible at any point in the pattern depending upon the direction of the stray signal in the QZ .

These plots show a discouraging result. Practice does not generally support the effect shown in these plots. As will be shown in section VII, the peak-to-peak amplitude and phase ripples seen in the QZ field are caused by many different stray signals from different spatial directions. The resultant uncertainty of these multiple signals is less (significantly so) than this maximum.

VI. EFFECTS OF AMPLITUDE TAPER

Independently, a parabolic amplitude taper is introduced for Q in equation (5), using values ranging from zero to 2 dB. The taper is superimposed onto the grid in Figure 2. The model of 1dB taper is shown in Figure 8.

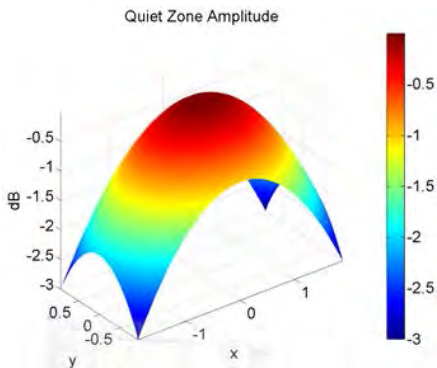


Figure 8. Introducing Amplitude Taper of 1dB

The resulting pattern in Figure 9 is compared to the ideal pattern. It can be seen that the taper depresses the first side lobe and widens the 3 dB beamwidth of the pattern. Figure 9 shows this comparing the ideal pattern to one with 1dB of induced taper. The subsequent table compares the ideal antenna parameters of interest to those with the various induced values of amplitude taper. The results predict reasonably accurate measurement of antenna parameters for a typical maximum amplitude taper requirement of 1 dB.

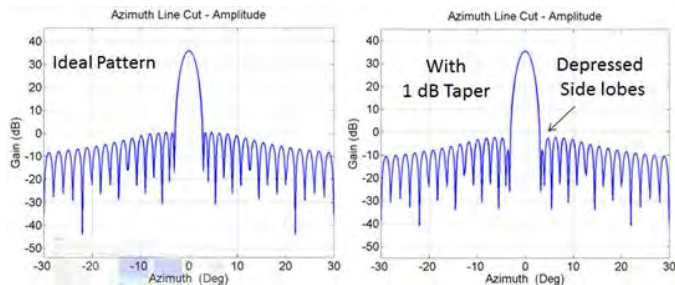


Figure 9. Results of Introducing Amplitude Taper

Antenna Parameter	With 0 dB Amplitude Taper	With 0.5 dB Amplitude Taper	With 1.0 dB Amplitude Taper	With 2.0 dB Amplitude Taper
Peak dB	35.6	35.8	35.4	35.7
3 dB Beamwidth	2.10	2.12	2.16	2.14
Peak Side Lobe dB _c	-35.3	-35.8	-34.3	-35.4

Table 1. Parametric Results of Inducing Taper

VII. ACTUAL COMPACT RANGE EXAMPLE

In a real compact range the imperfections in the illumination of the quiet zone will not be uniform nor from one source. It will be a combination consisting of stray signals throughout the range, surface deviations on the reflector, RF leakage and taper primarily from the compact range feed. A comprehensive field probing of a compact range will provide a composite and unique signature of the imperfections in the incident field of the quiet zone. A recent compact range installed and field probed by MI is used to demonstrate how Equation (5) can be used in conjunction with the field probe data to estimate or predict errors in subsequent antenna measurements. Radial field probe cuts were made at 15 degree intervals. The illuminating wave Q in Equation (5) is created by mapping the field probe data onto the grid of Figure 2, for the antenna of interest. Below are samples of some of the field probe measurements. The field probe cuts are not uniform in their amplitude and phase variation which is typical in a range. That is, it does not show a dominant stray signal.

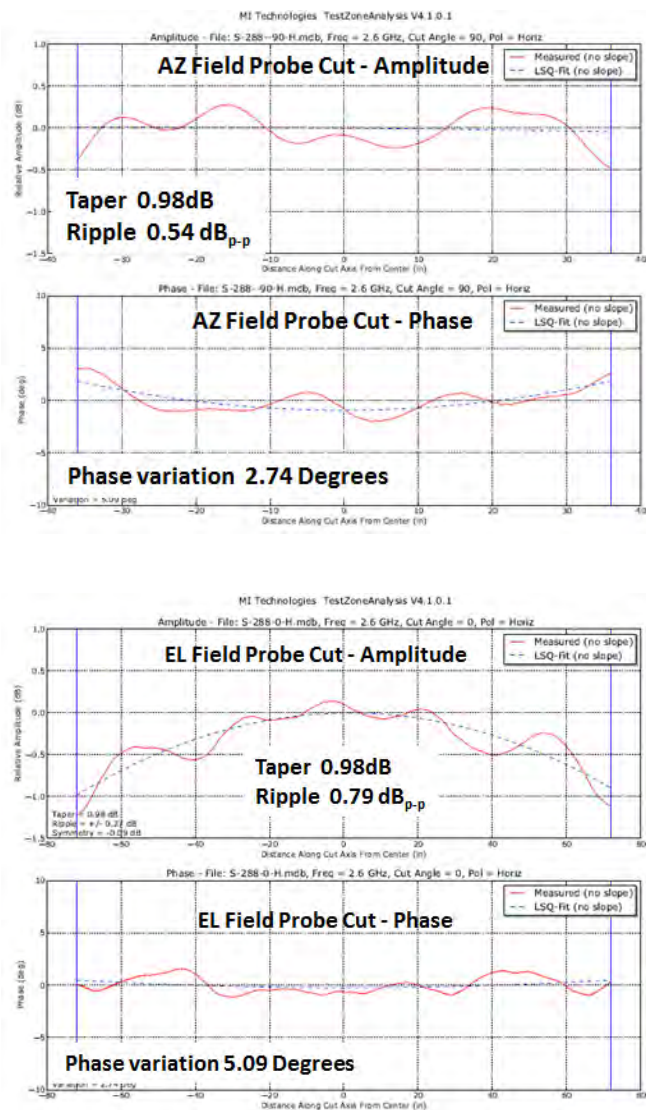


Figure 10. Example Measured Field Probe Data

The simulation is run resulting in the antenna pattern shown in Figure 11 and compared to the ideal case. The antenna pattern parameters are compared in the subsequent Table 2.

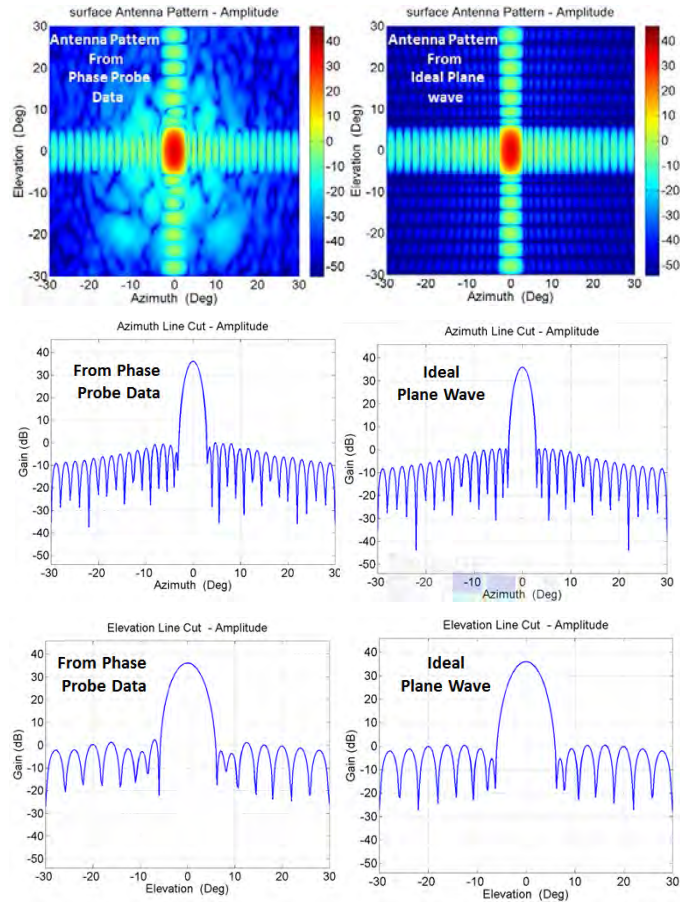


Figure 11. Antenna Pattern Comparison

Antenna Parameter	Ideal Antenna Pattern	Illuminated with Measured Non Ideal Plane Wave (From Phase Probe Data)
Peak dB	35.6	36.15
3 dB Beamwidth	2.10	2.13
Peak Side Lobe dB _c	-35.3	-33.5

Table 2. Antenna Pattern Parameters Comparison

The result predicts a much more accurate antenna measurement than the uncertainty bound calculated in section V and shown in Figure 7. This is more in line with the industry’s experience. Note Section V modeled single stray signals using the same values of measured amplitude ripple as shown in Figure 10, whereas Section VII used an illuminating field constructed by all the field probe cuts taking into account the total spectrum of variations contained therein.

VIII. SUMMARY

A method was shown to estimate antenna pattern parameter uncertainty from specified QZ metrics for a given ideal or expected antenna pattern. It was shown that the values of typical QZ specifications derived from field probe parameters can be inadequate to ensure acceptable measurements of antenna parameters if the source of the amplitude ripple and phase variation is a single stray signal. The method provides a worst case boundary condition that, while technically correct, is overly pessimistic in the typical compact range.

A method was shown to estimate antenna pattern measurement error using an expected antenna pattern and measured QZ field probe data from an existing compact range. The example predicted reasonable antenna measurement accuracy for that range. This same method can also be applied to predict performance using simulated QZ data when designing a compact range. This method can be very useful to evaluate the capability of a range to test candidate antennas or to evaluate the design of a new compact range reflector against a specified antenna using simulated QZ data. The method can be used to augment the typically specified field probe metrics.

Future work will investigate ways to adequately predict measurement uncertainty/error on a field probe cut by cut basis in lieu of constructing the entire illuminating field.

REFERENCES

- [1] Hollis, J.S., T.J. Lyon, and L. Clayton, Jr., eds., Microwave Antenna Measurements. Scientific-Atlanta, Inc., Atlanta, GA, November 1985.
- [2] T Lee, and W. Burnside, “Compact Range Reflector Edge Treatment Impact on Antenna and Scattering Measurements,” IEEE Trans., Antennas Propagat., vol. 45, pp 57-65, January 1997.